Journal of Low Temperature Physics
https://doi.org/10.1007/s10909-020-02388-4

A SQUID-Based Picovoltmeter for Quantum Resistors

Vidhi Shingla[1] · Ethan Kleinbaum[1] · Gábor A. Csáthy[1,2,3]

Received: 21 August 2019 / Accepted: 2 February 2020

Abstract
We present a sensitive voltage amplifier suited for measurements of source impedances in the kΩ range at dilution refrigerator temperatures. The circuit is based on a commercial dc SQUID, an impedance matching transformer, and it works on the principle of negative feedback. At 10 mK, the amplifier contribution to the noise is only 17 pV/$\sqrt{\text{Hz}}$, which is negligible in comparison with the fluctuations of the thermal voltage of a 3.25 kΩ metallic source resistor. Various circuit parameters of the amplifier are discussed.

Keywords Low-noise amplifier · dc SQUID · Quantum resistor

1 Introduction

In many applications, SQUIDs (Superconducting QUantum Interference Devices) are used as low-noise current amplifiers [1–3]. In such setups, the current to be measured is passed through an input coil and the magnetic field generated by this coil is efficiently coupled to the SQUID loop. Modern dc SQUIDs with the largest input coils achieve noise levels as low as 0.5 pA/$\sqrt{\text{Hz}}$ [2]. If in addition an impedance matching device is used, such as a transformer [4–15] or a cryogenic current comparator [16–23], noise levels of a few fA/$\sqrt{\text{Hz}}$ are accessible. Such sensitive current amplifiers are often used in high precision resistance bridges [16–23] and in noise thermometry [24–29].

SQUIDs can also be configured for voltage measurement [1]. Sensitive voltage amplifiers based on the principle of negative feedback were built first using early

Vidhi Shingla and Ethan Kleinbaum have contributed equally.

✉ Gábor A. Csáthy
gcsathy@purdue.edu

[1] Department of Physics and Astronomy, Purdue University, West Lafayette, IN 47907, USA

[2] Birck Nanotechnology Center, Purdue University, West Lafayette, IN 47907, USA

[3] Purdue Quantum Science and Engineering Institute, Purdue University, West Lafayette, IN 47907, USA

Published online: 13 February 2020

SQUID-like devices [30], rf SQUIDs [31–37], dc SQUIDs [38–40], and high T_c SQUIDs [41, 42]. In contrast to current amplifiers, voltage amplifiers have an input impedance greatly exceeding the resistance of the source to be measured.

Most SQUID-based voltmeters offer low-noise performance and sufficiently high input impedance for source resistors R_S in the mΩ–Ω range [31–35, 38–42]. However, numerous phenomena of interest occur in sources of resistance well into the kΩ range. Examples are the integer and fractional quantum Hall effect [43, 44], conduction phenomena in quantum point contacts [45], in topological insulators [46, 47], and the quantum anomalous Hall effect [48, 49], for which resistances are of the order of the quantum resistance $h/e^2 \simeq 25.8$ kΩ. The use of impedance matching transformers extended the use of SQUID-based voltage amplifiers for source resistances in the kΩ range, achieving noise levels of 0.8 nV/$\sqrt{\text{Hz}}$ [36] and 0.4 nV/$\sqrt{\text{Hz}}$ [37].

Here, we describe a SQUID-based voltage amplifier that is well-suited for low-noise measurements of quantum resistors. In contrast to other SQUID-based voltage amplifiers designed for source resistances in the kΩ range [36, 37], ours offer low-noise performance at dilution refrigerator temperatures, and it is based on a modern dc SQUID. We demonstrate low-noise operation by measuring voltage fluctuations in a source resistance $R_S = 3.25$ kΩ down to temperatures of 10 mK. At this temperature, the equivalent amplifier voltage noise is 17 pV/$\sqrt{\text{Hz}}$, significantly less than the Johnson noise of the source resistor. Measurements performed to frequencies as low as 1 Hz could not detect any significant $1/f$ noise. We also discuss other parameters of the voltage amplifier, such as its voltage gain, its bandwidth, and its input impedance.

2 Circuit Description

Our voltage amplifier, together with a voltage source V_{in} having a resistance $R_S = 3.25$ kΩ, is shown in Fig. 1. At the heart of the circuit, we used the combination of the dc SQUID and an impedance matching transformer [14]. As mentioned in the introduction, this combination of the dc SQUID and the transformer is a sensitive current amplifier for sources of resistance in the kΩ range. Our dc SQUID has an input coil with an inductance of $L_{\text{sq}} = 2.6$ μH. For our transformer, we opted for a coreless design [14]. The windings are of Nb wires. The secondary of the transformer is impedance matched to the SQUID input coil, and the two coils form a superconducting transformer. The impedance matching transformer has an effective turn ratio of 212, and it is mounted in a shielded formed of a combination of a cylindrical Pb tube and a soft magnetic shield. Further details of the behavior of the current amplifier formed of the combined dc SQUID and the impedance matching transformer can be found in Ref. [14].

In order to increase the input impedance necessary for voltage sensing, negative feedback is used [30–42]. The topology of our voltage amplifier circuit is similar to those in Refs. [32, 36, 37]. Negative feedback is realized by connecting the resistive divider formed of the resistors $R_F = 1$ MΩ and $R_G = 100$ Ω to the transformer

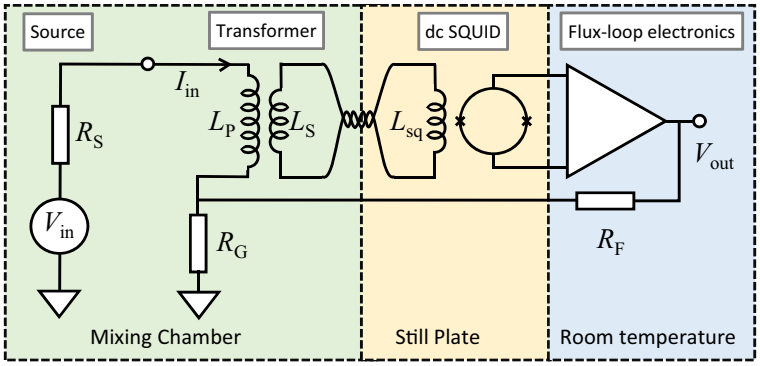

Fig. 1 Schematic of our sensitive voltage amplifier. The input coil of inductance L_{sq} of the dc SQUID is connected to an impedance matching transformer. In order to increase the impedance of the voltage sensing input, a negative feedback circuit is used that consists of resistors R_F and R_G. The mounting locations of various circuit elements within our dilution refrigerator are clearly marked (Color figure online)

primary winding, as shown in Fig. 1. Both resistors are of the thin metal film variety. Circuit elements are mounted onto various stages of a dilution refrigerator, as shown in Fig. 1. The feedback resistor R_F is at room temperature, whereas R_G and R_S are in close thermal contact with the mixing chamber. In addition, R_G is directly grounded to the mixing chamber.

For the proper functioning of our voltage amplifier, we implemented a few changes to the flux-loop electronics. When a dc SQUID is set up as a current amplifier, the modulation signal and the feedback signal from the output of the integrator are summed and are applied to the feedback coil of the SQUID [2]. Our current amplifier from Ref. [14] operates this way. In contrast, for the voltage amplifier shown in Fig. 1, the modulation and integrator output signals are separated. In our circuit, the modulation signal is still applied to the feedback coil (not shown in Fig. 1). However, the feedback signal V_{out} from the output of the integrator is no longer fed into the feedback coil; it is instead connected to R_F of the resistive feedback circuit. The programmable feedback loop circuit model PFL-100 we use allows for an easy separation of the two signals at the flip of a switch [50]. Furthermore, we found that a stable flux locking for the voltage amplifier circuit could not be achieved with the existing integrator capacitors; we modified one of the factory provided settings to 11 µF.

The flux-locked operation of the SQUID within the voltage amplifier still ensures a constant flux in the SQUID loop and therefore a linear operation. However, the change to the feedback path described above is expected to change the transimpedance gain of the chain of transformer, SQUID, and flux-loop electronics. In Fig. 2a, we show a model of our voltage amplifier in which the chain of transformer, SQUID and flux-loop electronics was replaced by a current-controlled voltage source with a transimpedance gain $\tilde{R}_T = V_{out}/I_{in}$. For the programmable feedback loop circuit model PFL-100 we use, we measured $\tilde{R}_T = 67$ GΩ. We note that this value exceeds that corresponding to the same circuit elements but with the feedback of the summed

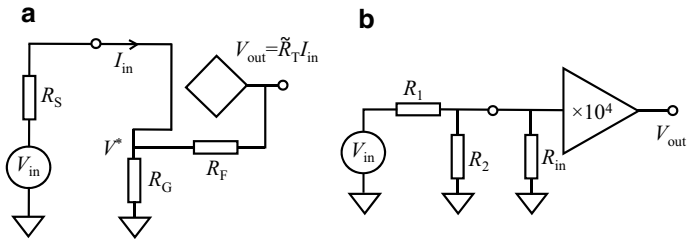

Fig. 2 **a** A circuit model for the voltage amplifier. At the heart of this model, there is a current-controlled voltage source with a transimpedance gain $\tilde{R}_T$ as well as a resistive feedback circuit composed of R_F and R_G. **b** Circuit used to measure the input resistance of our amplifier R_{in}

up modulation and integrator signals applied to the modulation coil by about a factor 30 [14].

3 Circuit Analysis

The operation of voltage feedback amplifiers was discussed in detail in Refs. [31, 32]. In order to understand our circuit far below its bandwidth, we will use the simplified circuit model shown in Fig. 2a. Kirchhoff's voltage law applied to the input circuit of this model yields $V_{in} - R_S I_{in} = V^*$. Kirchhoff's law for currents at the feedback node is $I_{in} + (V_{out} - V^*)/R_F = V^*/R_G$. Here, V^* is the voltage of the feedback node. By solving these equations in the limit of $\tilde{R}_T \geq R_F \geq R_S \geq R_G$, we obtain

$$G = \frac{V_{out}}{V_{in}} = \frac{R_F}{R_G}\left(1 + \frac{R_F R_S}{R_G \tilde{R}_T}\right)^{-1} \simeq \frac{R_F}{R_G}. \tag{1}$$

For our choice of resistors, the voltage gain is $G = 10^4$. The term containing the source resistance has a negligible effect on the value of the gain. For the resistors used in our circuit, this term contributes less than 0.1% error to the gain.

Besides the voltage gain, another parameter to be considered is the equivalent input resistance R_{in}. An equivalent circuit of our amplifier that contains the input resistance is shown on the right-hand side of Fig. 2b. The input resistance can be estimated as follows:

$$R_{in} = \frac{V_{in}}{I_{in}} = \frac{V_{in}}{V_{out}}\frac{V_{out}}{I_{in}} = \frac{\tilde{R}_T}{G} \simeq \frac{\tilde{R}_T R_G}{R_F}. \tag{2}$$

Using the circuit shown in Fig. 2b, we measured the input resistance. With $R_1 = 10$ MΩ, $R_2 = 1$ MΩ, and at an input voltage of 100 μV, the measured output was 80 mV. Therefore, the estimated input resistance is $R_{in} = 6.7$ MΩ. This value is in excellent agreement with the expected values from the equation above, and it is three orders of magnitude larger than our source resistance. Such a large input

resistance assures that our amplifier is voltage sensing. We note that within our model, the input resistance is independent of the source resistance.

The gain equation, Eq. 1, can also be used to estimate the bandwidth of the circuit. If instead of a constant transimpedance gain, we consider a single-pole low-pass frequency response for the transimpedance gain for the current-controlled voltage source $\tilde{R}_T \rightarrow \tilde{R}_T(1 + jf/f_0)$, with $f_0 = 5$ Hz, the bandwidth Bw of the voltage amplifier may be expressed as

$$\mathrm{Bw} = f_0 \frac{R_G \tilde{R}_T}{R_F R_\mathrm{S}}. \tag{3}$$

We thus find that in contrast to transistor-based and operation amplifier-based voltage amplifiers, our amplifier has a bandwidth that is a strong function of the source resistance. Numerical values for our circuit result in a bandwidth of 10 kHz or a gain-bandwidth product of 10^8 Hz. We note the inductance of the transformer primary may also limit the bandwidth. However, in our circuit, this effect occurs at frequencies much larger than 10 kHz and may be safely ignored.

4 Noise Model and Noise Measurement

In order to obtain the input-referred voltage noise e_in of the circuit shown in Fig. 1, we will consider the noise generated by each circuit element of our amplifier. The noise has two major components: the Johnson noise generated by the source resistor $e_{J,R_\mathrm{S}} = (4k_\mathrm{B}TR_\mathrm{S})^{1/2}$ and the noise added by the amplifier e_amp:

$$e_\mathrm{in}^2 = e_{J,R_\mathrm{S}}^2 + e_\mathrm{amp}^2 \tag{4}$$

Here, we used the fact that noises add in quadrature and denoted by k_B the Boltzmann constant, and by T the temperature of the source resistor. In our setup, the source resistor is in thermal contact with the mixing chamber.

Amplifiers have a voltage and current noise, e_a and i_a, respectively. The amplifier noise is then expressed as

$$e_\mathrm{amp}^2 = e_a^2 + (i_a R_\mathrm{S})^2. \tag{5}$$

We recall that within the simplest description, the noise of the transimpedance amplifier composed of the transformer, SQUID, and flux-locked electronics chain can be modeled with a single noise source $i_a = 2.3\ \mathrm{fA}/\sqrt{\mathrm{Hz}}$ [14]. This current noise is referred to the primary of the transformer L_P , and it is thus identical to the current noise of the amplifier. The voltage noise of the amplifier, within our model, is due to the Johnson noise of the feedback resistors: $e_a^2 = e_{J,R_G}^2 + e_{J,R_F}^2/G^2 = 4k_\mathrm{B}TR_G + 4k_\mathrm{B}T_\mathrm{room}R_F/G^2$. Here, we took into account that R_F is at room temperature T_room and its noise adds to the amplifier output; hence, its input-referred contribution must be divided by the voltage gain G.

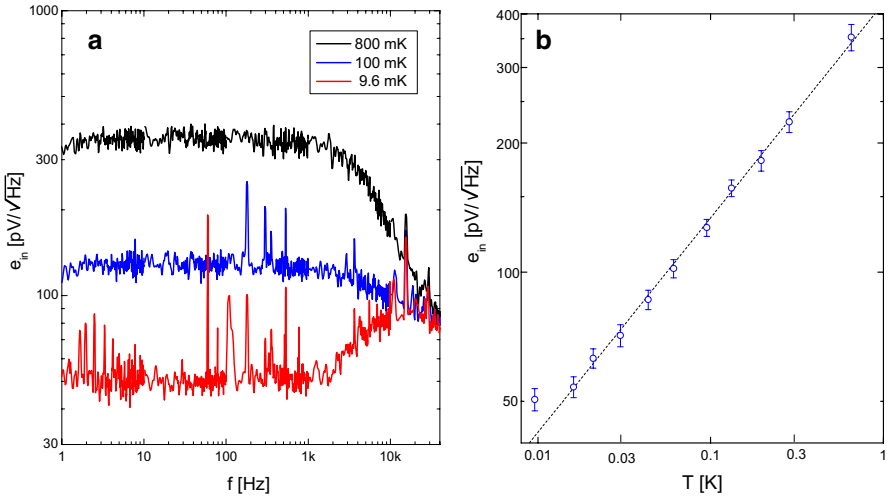

Fig. 3 **a** The frequency dependence of the noise voltage $e_{\rm in}$ at three selected temperatures of the mixing chamber. **b** Data points show the temperature dependence of the measured noise voltage $e_{\rm in}$. Dashed line indicates the calculated Johnson noise for the source resistor. Measured values of the noise $e_{\rm in}$ are in excellent agreement with the Johnson noise of the source resistor $e_{J,R_{\rm S}}$, indicating therefore that the noise contribution of the amplifier is negligible (Color figure online)

Based on the noise model described above, the noise components for our circuit calculated at $T = 10$ mK are $e_{J,R_{\rm S}} = 42\,{\rm pV}/\sqrt{\rm Hz}$, $e_{\rm amp} = 17\,{\rm pV}/\sqrt{\rm Hz}$, and $e_{\rm in} = 46\,{\rm pV}/\sqrt{\rm Hz}$. At this and other higher temperatures of the mixing chamber, the amplifier noise is significantly less than the Johnson noise of the source resistor. Therefore, our amplifier is suitable for measurements of the fluctuations of the thermal voltage at dilution refrigerator temperatures. In Fig. 3a, we show the frequency dependence of the measured voltage noise $e_{\rm in}$ at three representative temperatures. The plotted quantity is $e_{\rm in} = e_{\rm out}/G$, the noise voltage measured at the amplifier output divided by the voltage gain G of the amplifier. With the exception of the 60 Hz coherent interference and pickup of cryostat vibrations, the measured noise is white, i.e., frequency independent up to about 2 kHz. We note the absence of any significant $1/f$ noise component down to a frequency of 1 Hz. A comparison of the measured voltage noise $e_{\rm in}$ and of the Johnson noise $e_{J,R_{\rm S}}$ of the source resistor $R_{\rm S}$, shown in Fig. 3b, reveals a good agreement over a wide temperature range, down to about 20 mK. This means that the amplifier indeed adds negligible noise, and it demonstrates that the amplifier can be used for Johnson noise measurement at dilution refrigerator temperatures.

Also shown in Fig. 3b, our measurement at 9.6 mK exhibits a clear deviation of the input-referred noise $e_{\rm in}$ from the Johnson noise $e_{J,R_{\rm S}}$ of the source resistor calculated at this temperature. Such a deviation is often observed in measurements performed at low mK temperatures, and it is commonly attributed to a lack of full thermalization of the source resistor. Within the noise model used, we estimated earlier the amplifier noise $e_{\rm amp}$ at 10 mK to be about a factor of 2.5 less than the Johnson noise of the source resistor $e_{J,R_{\rm S}}$ calculated at 10 mK. This means that back-action

heating is insufficient to account for the lack of thermalization of source resistor at the lowest temperatures. We then surmise that a combination of the coherent noise pickup and of microwave heating is likely the explanation for the loss of thermalization of the source resistor observed near 10 mK. Quantitative estimations of the power leakage may be obtained after gaining knowledge about the effective thermal resistance of the source resistor. Such estimations are often enabled by self-heating measurements of the source resistor. However, such self-heating measurements require the use of additional wires necessary for resistor biasing, which may change the residual power leakage. Therefore, these biasing wires must be carefully filtered.

We estimate that the Johnson noise of the source resistor becomes equal to the amplifier noise at $R_S \simeq 100\,\text{k}\Omega$, thus our voltage amplifier is useful for resistors in the kΩ range, a range that encompasses the quantum resistance $h/e^2 \simeq 25.8\,\text{k}\Omega$.

The noise model used justifies the need for an impedance matching transformer in our circuit. If the dc SQUID is used without a transformer, the current noise referred to the SQUID pickup coil L_{sq} is $i_a \simeq 0.5\,\text{pA}/\sqrt{\text{Hz}}$ [14]. Such a current noise increases significantly the value of $i_a R_S$ term in the amplifier noise and adversely affects low-noise operation for kΩ valued source resistors. Voltage amplifier circuits with no impedance matching transformers, however, have good noise performance for $R_S \ll 1\,\Omega$ [31–35, 38–42].

An unusual feature of the measured noise spectrum at 9.6 mK is the increasing trend with frequency past 2 kHz. This trend may be observed in the lowest temperature data in Fig. 3a. We think that a noise term with such a frequency dependence is generated when the noise current passes through the inductance of the transformer primary: $i_a \omega L_{\text{eff}}$. This noise term calculated with $L_{\text{eff}} = 0.87$ H of our transformer [14] offers a quantitative explanation for the noise increase at the largest frequencies measured near the base temperature of our fridge.

To conclude, we presented a sensitive voltage amplifier circuit suitable for measurements of picovolt level signals in kΩ level resistors at dilution refrigerator temperatures. The input resistance of the amplifier was measured to be 6.7 MΩ and for a source resistance of 3.25 kΩ , the bandwidth of the amplifier was found about 10 kHz. A simple circuit model was used to explain a variety of circuit parameters. We also demonstrated measurements of the thermal fluctuations of the voltage in a $R_S = 3.25\,\text{k}\Omega$ source resistor.

Acknowledgements We thank Dr. Robin Cantor of Star Cryoelectronics for kindly sharing information about the flux-lock electronics. This work was supported by the US NSF Grants No. DMR 1505866 and 1904497.

References

1. J. Clarke, Philos. Mag. **13**, 115 (1966)
2. J. Clarke, A.I. Braginski, *The SQUID Handbook* (Wiley, New York, 2004)
3. D. Drung, C. Assmann, J. Beyer, A. Kirste, M. Peters, F. Ruede, Th Schurig, I.E.E.E. Trans, Appl. Supercond. **17**, 699 (2007)
4. J. Clarke, W.E. Tennant, D. Woody, J. Appl. Phys. **42**, 3859 (1971)

5. S. Barbanera, P. Carelli, I. Modena, G.L. Romani, J. Appl. Phys. **49**, 905 (1978)
6. S.Q. Xue, P. Gutmann, V. Kose, Rev. Sci. Instrum. **52**, 1901 (1981)
7. P. Gutmann, V. Kose, IEEE Trans. Instrum. Meas. **IM–36**, 267 (1987)
8. M. Tarasov, A. Kalabukhov, S. Kovtonjuk, I. Lapitskaya, S. Gudoshnikov, M. Kiviranta, O. Snigirev, L. Kuzmin, J. Commun. Technol. Electron. **48**, 1404 (2003)
9. V. Polushkin, E.G.D. Glowacka, D. Goldie, J. Lumley, Physica C **367**, 280 (2002)
10. C. Granata, A. Vettoliere, M. Russo, Rev. Sci. Instrum. **82**, 013901 (2011)
11. J. Luomahaara, M. Kiviranta, J. Hassel, Supercond. Sci. Technol. **25**, 035006 (2012)
12. V. Zakosarenko, M. Schmelz, R. Stolz, T. Schönau, L. Fritzsch, S. Anders, H.G. Meyer, Supercond. Sci. Technol. **25**, 095014 (2012)
13. J. Luomahaara, A. Kemppinen, P. Helistö, J. Hassel, I.E.E.E. Trans, Appl. Supercond. **23**, 1601705 (2013)
14. E. Kleinbaum, V. Shingla, G.A. Csáthy, Rev. Sci. Instrum. **88**, 034902 (2017)
15. V. Shingla, E. Kleinbaum, L.N. Pfeiffer, K.W. West, G.A. Csáthy, Meas. Sci. Technol. **29**, 105903 (2018)
16. F. Gay, F. Piquemal, G. Genevès, Rev. Sci. Instrum. **71**, 4592 (2000)
17. T.J.B.M. Janssen, A. Hartland, IEEE Proc. Sci. Meas. Technol. **147**, 174 (2000)
18. G. Rietveld, E. Bartolomé, J. Sesé, P. de la Court, J. Flokstra, C. Rillo, A. Camón, IEEE Trans. Instrum. Meas. **52**, 621 (2003)
19. R.E. Elmquist, E. Hourdakis, D.G. Jarrett, N.M. Zimmerman, IEEE Trans. Instrum. Meas. **54**, 525 (2005)
20. G. Rietveld, P. de la Court, H.E. von den Brom, IEEE Trans. Instrum. Meas. **58**, 1196 (2009)
21. L. Devoille, N. Feltin, B. Stock, B. Chenaud, S. Sassine, D. Djordevic, O. Séron, F. Piquemal, Meas. Sci. Technol. **23**, 124011 (2012)
22. F. Rengez, O. Séron, L. Devoille, D. Placko, F. Piquemal, in *Proceedings of Conference on Precision Electromagnetic Measurements CPEM 2014* (2014), p. 296
23. M. Götz, E. Pesel, D. Drung, in *Proceedings of Conference on Precision Electromagnetic Measurements CPEM 2014* (2014), p. 684
24. R.A. Kamper, J.E. Zimmerman, J. Appl. Phys. **42**, 132 (1971)
25. R.A. Webb, R.P. Giffard, J.C. Wheatley, J. Low Temp. Phys. **13**, 383 (1973)
26. M.L. Roukes, M.R. Freeman, R.S. Germain, R.C. Richardson, M.B. Ketchen, Phys. Rev. Lett. **55**, 422 (1985)
27. C.P. Lusher, J. Li, V.A. Maidanov, M.E. Digby, H. Dyball, A. Casey, J. Nyéki, V.V. Dmitriev, B.P. Cowan, J. Saunders, Meas. Sci. Technol. **12**, 1 (2001)
28. A. Casey, F. Arnold, I.V. Levitin, C.P. Lusher, J. Nyéki, J. Saunders, A. Shibahara, H. van der Vliet, B. Yager, D. Drung, Th Schurig, G. Batey, M.N. Cuthbert, A.J. Matthews, J. Low Temp. Phys. **175**, 764 (2014)
29. A. Shibahara, O. Hahtela, J. Engert, H. van der Vliet, L.V. Levitin, A. Casey, C.P. Lucher, J. Saunders, D. Drung, Th Schurig, Philos. Trans. R. Soc. A **374**, 20150054 (2016)
30. J.W. McWane, J.E. Neighbor, R.S. Newbower, Rev. Sci. Instrum. **37**, 1602 (1966)
31. R.P. Giffard, R.A. Webb, J.C. Wheatley, J. Low Temp. Phys. **6**, 533 (1972)
32. A. Davidson, R.S. Newbower, M.R. Beasley, Rev. Sci. Instrum. **45**, 838 (1974)
33. R.H. Dee, A.M. Guènault, G.R. Pickett, J. Phys. E Sci. Instrum. **9**, 807 (1976)
34. L. Smrčka, P. Středa, P. Svoboda, Cryongenics **18**, 670 (1978)
35. T. Fujita, T. Ohtsuka, Jpn. J. Appl. Phys. **15**, 881 (1976)
36. F. Delahaye, D. Bournaud, IEEE Trans. Instrum. Meas. **40**, 237 (1991)
37. M. Nakanishi, Jpn. J. Appl. Phys. **43**, 7307 (2004)
38. V. Polushkin, D. Drung, H. Koch, Rev. Sci. Instrum. **65**, 3005 (1994)
39. F. Sachslehner, W. Vodel, Cryogenics **38**, 293 (1998)
40. L. Saury, in *Proceedings of Conference on Precision Electromagnetic Measurements CPEM 2000* (2000), p. 671
41. A.H. Milklich, D. Koelle, F. Ludwig, D.T. Nemeth, E. Dantsker, J. Clarke, Appl. Phys. Lett. **66**, 230 (1995)
42. T. Erikkson, J. Blomgren, D. Winkler, T. Holst, Y.Q. Shen, I.E.E.E. Trans, Appl. Supercond. **9**, 3495 (1999)
43. K. von Klitzing, G. Dorda, M. Pepper, Phys. Rev. Lett. **45**, 494 (1980)
44. D.C. Tsui, H.L. Stormer, A.C. Gossard, Phys. Rev. Lett. **48**, 1559 (1982)

45. B.J. van Wees, H. van Houten, C.W.J. Beenakker, J.G. Williamson, L.P. Kouwenhoven, D. van der Marel, C.T. Foxon, Phys. Rev. Lett. **60**, 848 (1988)
46. M. König, S. Wiedmann, C. Brüne, A. Roth, H. Buhmann, L.W. Molenkamp, X.-L. Qi, S.-C. Zhang, Science **318**, 766 (2007)
47. L. Du, I. Knez, G. Sullivan, R.R. Du, Phys. Rev. Lett. **114**, 096802 (2015)
48. C.-Z. Chang, J. Zhang, X. Feng, J. Shen, Z. Zhang, M. Guo, K. Li, Y. Ou, P. Wei, L.-L. Wang, Z.-Q. Ji, Y. Feng, S. Ji, X. Chen, J. Jia, X. Dai, Z. Fang, S.-C. Zhang, K. He, Y. Wang, L. Lu, X.-C. Ma, Q.-K. Xue, Science **340**, 167 (2013)
49. C.-Z. Chang, W. Zhao, D.Y. Kim, H. Zhang, B.A. Assaf, D. Heiman, S.-C. Zhang, C. Liu, M.H.W. Chan, J.S. Moodera, Nat. Mater. **14**, 473 (2015)
50. STAR Cryoelectronics model SQ2600